International Communications in Heat and Mass Transfer 39 (2012) 923–930

Contents lists available at SciVerse ScienceDirect

International Communications in Heat and Mass Transfer

journal homepage: www.elsevier.com/locate/ichmt

Theoretical study of oscillatory phenomena in a horizontal closed-loop pulsating heat pipe with asymmetrical arrayed minichannel ☆

Ching-Ming Chiang [a], Kuo-Hsiang Chien [b], Han-Ming Chen [a], Chi-Chuan Wang [c,*]

[a] Department of Mechanical Engineering, National Taiwan University, Taipei, Taiwan
[b] Green Energy and Environment Research Laboratories, Industrial Technology Research Institute, Hsinchu, Taiwan
[c] Department of Mechanical Engineering, National Chiao-Tung University, Hsinchu, Taiwan

ARTICLE INFO

Available online 2 June 2012

Keywords:
Pulsating heat pipe
Asymmetrical arrayed minichannel
Number of turns
Filled liquid ratio
Frequency ratio

ABSTRACT

This study develops an analytical model applicable for predicting the oscillatory motion of a pulsating heat pipe (PHP) with asymmetrical arrayed minichannel configuration. The analytic model takes into account the temperature difference between the average evaporating region and the average condensing region as the thermally driven force for the oscillatory motion. It is found that the dominant parameters affecting the PHP include configurations and dimensions of the flow channel, the number of turns, the filled liquid ratio, the frequency ratio, the operating temperature, and the temperature difference between the average evaporating region and the average condensing region are investigated in this study. The calculated results show that the closed-loop pulsating heat pipe with asymmetrical arrayed minichannel under lower number of turns, lower filled liquid ratio, higher operating temperature and higher temperature difference between the average evaporating region and the average condensing region for the frequency ratio of unity could attain a better performance of the oscillatory motions.

1. Introduction

With continuous shrinkage of integrated circuits and endless rising of capability/functions of electronic devices, the dissipating power of internal chip array is also substantially increased accordingly. Hence, with efficient heat removal from the electronic devices, damage or even failure of the whole system is evitable. It is therefore imperative to provide an efficient cooling technique to meet the rising demand for the current electronic industry.

One of the novel designs for effective heat removal is the pulsating heat pipe which was originally proposed by Akachi [1]. The pulsating heat pipe (PHP) or called the oscillating heat pipe (OHP) is made of slender tubes having serpentine configurations. By filling appropriate amount of working fluid into PHP, the PHPs are able to function properly with liquid slugs and vapor plugs being distributed arbitrarily and unevenly within the whole tube. In an effort to avoid the shortcoming of stratified flow, Cai et al. [2] suggested that the interior diameter should not be larger than 3 mm.

In general, the PHP have three types: (1) the closed-loop type, which has two ends interconnected with each other and the working fluid could be circulated in the tube; (2) the closed-loop with check valve type, in which flow direction of the working fluid could be controlled; (3) the closed-end type, which has two ends sealed off and only fluid flow without circulation in the tube. Zhang et al. [3] experimentally investigated the closed-loop PHP and showed that a better thermal performance than that of the closed-end. The closed-loop PHP with check valve is not popular because installing the check valve is normally accompanied with much higher expense. As a result, the closed-loop PHP is often regarded as the most probable candidates as far as PHP is concerned. Note that the closed-loop PHP is a passive device which can be used in the absence of any external or electrical powers. Some of the main advantages of the closed-loop PHP when compared to the conventional heat pipe are the absence of the wick structure and the ability to transport heat to sufficient long distance.

The closed-loop PHP is composed of the evaporating, condensing and adiabatic regions during normal operation. The evaporating and condensing regions are the regimes of the received and removed heat, respectively. The adiabatic region between the evaporating and condensing region is optional in terms of practical application. There were considerable studies concerning the performance of PHP either experimentally or theoretically. For instance, the effects of hydraulic diameter, the number of turns, working fluids, filling liquid ratio, inclined angles, and heat transfer rate on the performance of PHP were reported by Refs. [2,4–12], Refs. [4,7,13], Refs. [3,4,8–10], Refs. [2–4,6,8,9,11–13], Refs. [5,7], and Refs. [2,3,5,7,10–12], respectively. A detailed review about the relevant researches was summarized by Zhang and Faghri [14]. Besides, the impinging jets can be used to cooling high heat flux of the electronic devices. The fluidic flow and heat transfer associated with pulsating impinging jets were numerically analyzed by Refs.

☆ Communicated by W.J. Minkowycz.

* Corresponding author at: EE474, 1001 University Road, Hsinchu, Taiwan 300.
E-mail address: ccwang@mail.nctu.edu.tw (C-C. Wang).

0735-1933/$ – see front matter © 2012 Elsevier Ltd. All rights reserved.
doi:10.1016/j.icheatmasstransfer.2012.05.019

Nomenclature

A	cross-sectional area (m^2)
a	channel width (m)
B	perimeter (m)
c	damping coefficient ($N\,s\,m^{-1}$)
D_h	hydraulic diameter (m)
F	force (N)
F_c	capillary force (N)
F_d	driving force (N)
F_f	frictional force (N)
F_i	inertial force (N)
F_v	elastic restoring force (N)
f	friction factor
f_n	undamped natural frequency (Hz)
G	magnitude of driving force (N)
h_{fg}	latent heat of vaporization ($J\,kg^{-1}$)
k	spring stiffness ($N\,m^{-1}$)
L	length (m)
m	mass (kg)
N	number of turns
P	pressure ($N\,m^{-2}$)
R	gas constant ($J\,kg^{-1}\,K^{-1}$)
Re	Reynolds number
S	capillary force (N)
T	temperature (°C)
t	time (s)
V	volume (m^3)
x	coordinate (m)

Greek symbols

γ	frequency ratio
ΔT	temperature difference between the average evaporating region and the average condensing region (°C)
ζ	damping ratio
θ_a	dynamic contact angle of advancing (°)
θ_r	dynamic contact angle of receding (°)
μ	dynamic viscosity ($kg\,m^{-1}\,s^{-1}$)
ρ	density ($kg\,m^{-3}$)
σ	surface tension ($N\,m^{-1}$)
φ	filled liquid ratio (%)
ω	driving frequency ($rad\,s^{-1}$)
ω_n	undamped natural frequency ($rad\,s^{-1}$)

Subscripts

a	adiabatic region
c	condensing region
e	evaporating region
i	small flow channel
j	big flow channel
l	liquid slug
r	reference
sat	saturated
t	total
v	vapor plug

[15,16]. Yen et al. [17] simulated the effects of the amplitude, frequency, permeability of the porous block, and porous blockage ratio that affect the pulsating flow in a channel with a porous-block-mounted heat source. The lid-driven cavity has been found in electronic cooling for practical application. Aminossadati and Ghasemi [18] formulated a two-dimensional square cavity under unsteady laminar mixed convection flow. They showed that the average heat transfer rate of the cavity with an oscillating wall is lower than that of a constant velocity wall for low Richardson number.

Despite some efforts that had been undertaken, there is still a need for detailed physical interpretation of this process subject to influencing parameters. This is because the flow oscillatory phenomenon in a closed-loop PHP is rather complex. Some dominant mechanisms for this process includes configurations and dimensions of the flow channel, the number of turns, the filled liquid ratio, the frequency ratio, the operating temperature, the temperature difference between the average evaporating region and the average condensing region, the combination of working fluid with channel material, and the dynamic contact angle of advancing with receding. Nevertheless, the complicated relationships between these effects have not been completely investigated. It is therefore crucial to conduct parametric study on the oscillatory phenomena in a closed-loop PHP. To attain the better uniformity of temperature and higher capability of heat transport, the closed-loop PHP with asymmetrical arrayed minichannel is adopted. The advantages of the closed-loop PHP with asymmetrical arrayed minichannel can be validated by comparing its performance with that having constant cross-sectional area for creating more unbalancing capillary force to boost the PHP. Hence, the objective of this study is to develop an analytical model for predicting the oscillation motion in a pulsating heat pipe with and without asymmetrical arrayed minichannel pertaining to horizontal arrangement.

2. Theoretical model

Fig. 1(a) denotes a schematic with detailed dimension for the present modeling. The closed-loop PHP contains an evaporating and a condensing region with an adiabatic region in between. The saturated liquid slugs and vapor plugs are distributed arbitrarily and unevenly in the closed-loop PHP as shown in Fig. 1(a). The evaporating region of the closed-loop PHP received external heat input during the operation, and the working fluid absorbs heat from the channel wall. This basic modeling is similar to that of Ma et al. [8] but with a much more comprehensive revision. The basic assumptions are as follows:

(1) The PHP is a closed-loop type and operates horizontally with little influence of gravity.
(2) The liquid slug is incompressible and the vapor plug is assumed to behave as an ideal gas.
(3) Both liquid slug and vapor plug flowing in the channel are considered one-dimensional.
(4) Fully developed laminar flow prevails along the channel.
(5) The minor pressure losses including the bends, gradual expansion and contraction sections are negligible.
(6) The heat transfer between the liquid slug, vapor plug and channel wall is not considered.
(7) The influence of liquid film and the shear force along the liquid/vapor interface is negligible.
(8) The capillary force along the flow path is assumed to be constant.
(9) The closed-loop PHP is constituted of rectangular minichannel with two cross-sectional areas as shown in Fig. 1(a).

As evaporating region received the heat from surroundings, the saturated temperature and pressure are described by the Clapeyron–Clausius equation:

$$\ln\left(\frac{P_e}{P_r}\right)_{sat} \cong \frac{h_{fg}}{R}\left(\frac{1}{T_r}-\frac{1}{T_e}\right)_{sat}. \quad (1)$$

The foregoing relationship is also applicable to the condensing region. This can be done by expanding Eq. (1) using Taylor series and introducing ideal gas equation of state, and neglecting the higher order terms from this operation. Hence, the pressure

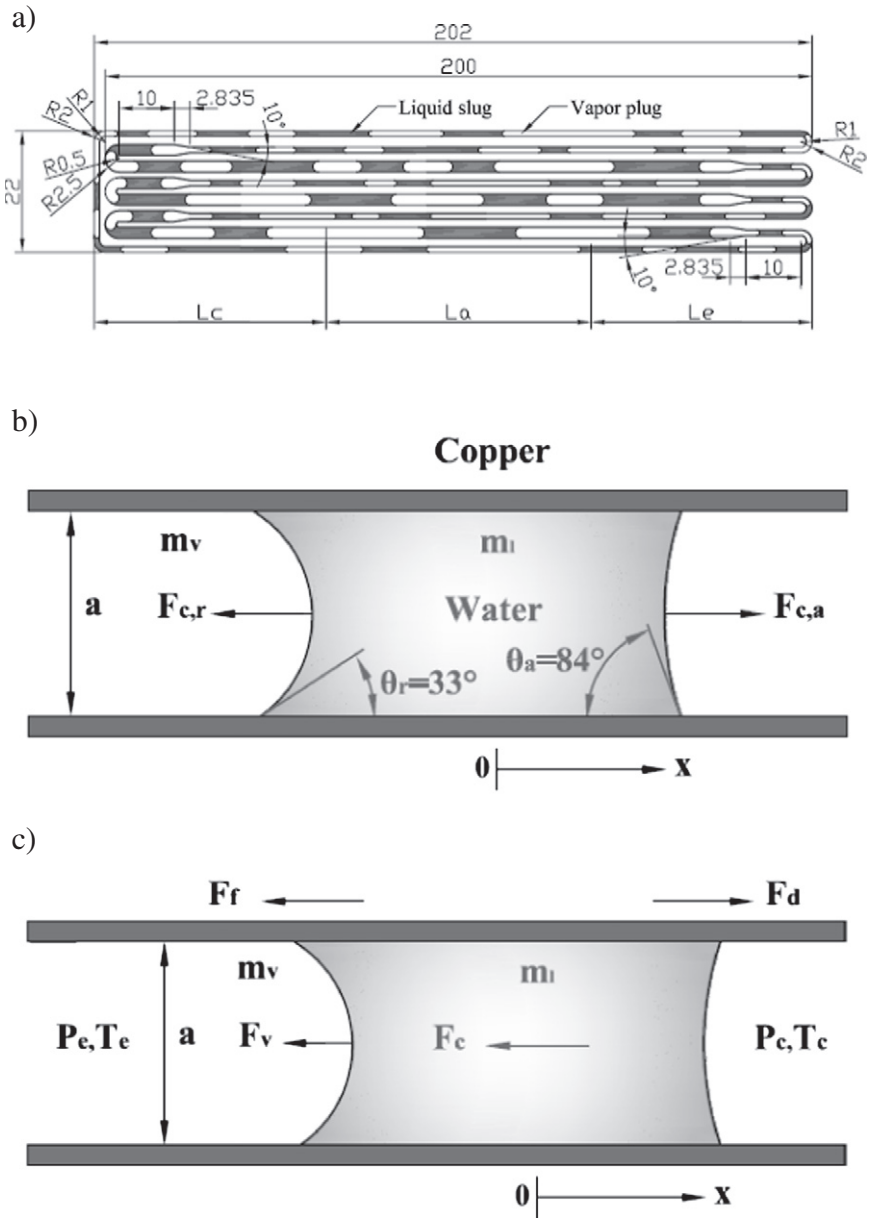

Fig. 1. Schematic of a closed-loop PHP model. (a) The closed-loop PHP with asymmetrical arrayed minichannel (all dimensions with out of scale are in mm). (b) The capillary force and dynamic contact angle along the flow path. (c) The individual forces.

difference between the evaporating and condensing region can be rearranged as

$$P_e - P_c = \frac{h_{fg}\rho_{v,c}}{T_e}(T_e - T_c). \tag{2}$$

However, the heat input into the evaporating region leads to an increase of saturated temperature and consequently the expansion of vapor plug. The heat output from the condensing region leads to a decrease of temperature and the contraction of vapor plug. The evaporation and condensation processes brought about the oscillatory motion in the closed-loop PHP. In addition, it is expected that the evaporating and condensing temperature varies along the evaporator and condenser. With a prescribed driving frequency of ω, the temperature difference between the average evaporating region and the average condensing region can be re-written as

$$T_e - T_c = \frac{(\bar{T}_e - \bar{T}_c)}{2}(1 + \cos\omega t). \tag{3}$$

By combining Eqs. (2) and (3), the thermally driven force for the oscillatory motion with regard to asymmetrical arrayed minichannel can be obtained by

$$F_d = \left[\frac{h_{fg}\rho_{v,c}}{2T_e}\left(A_i + A_j\right)(\bar{T}_e - \bar{T}_c)\right](1 + cos\omega t), \tag{4}$$

where A_i and A_j are the cross-sectional area of different flow channels.

The oscillatory flow starting up inside the horizontal channel and the pressure gradient along the flow path can be readily calculated by

$$\frac{dP}{dx} = \frac{f\rho}{2D_h}\left(\frac{dx}{dt}\right)^2. \tag{5}$$

The frictional force stemming from fluid flow in the asymmetrical arrayed minichannel can be evaluated by integrating Eq. (5). Thus,

$$F_f = \left\{ \frac{NV_i}{2D_{h,i}^2}\left\{(f_l\cdot Re_l)_i\phi\mu_l + (f_v\cdot Re_v)_i[(1-\phi)\mu_v]\right\} + \frac{NV_j}{2D_{h,j}^2}\left\{(f_l\cdot Re_l)_j\phi\mu_l + (f_v\cdot Re_v)_j[(1-\phi)\mu_v]\right\}\right\}\frac{dx}{dt}, \tag{6}$$

where φ is the filled liquid ratio, representing the volume of the working fluid relative to the total volume inside the closed-loop PHP, viz. $\varphi = V_l/V_t$.

As stated before, the variation of the pressure difference of vapor plug is linear along the flow path with ideal gas behavior. For this reason, the required work subject to expansion and compression processes of the vapor plug can be determined by

$$F_v = \left[\frac{\rho_v RT}{(1-\phi)}\left(\frac{A_i^2}{NV_i} + \frac{A_j^2}{NV_j}\right)\right]x. \tag{7}$$

The interface divided by the liquid slug and vapor plug is called the meniscus as shown in Fig. 1(b). From Faghri [19], the dynamic contact angle of advancing and receding are $\theta_a = 84°$ and $\theta_r = 33°$, respectively, and is also depicted in Fig. 1(b). Based on the Laplace equation, the capillary force for asymmetrical arrayed minichannel can be found as

$$F_c = F_{c,a} - F_{c,r} = \sigma(\cos\theta_a - \cos\theta_r)\left(B_i + B_j\right). \tag{8}$$

3. Governing equation with parametric designs

Fig. 1(c) illustrates the interaction of the individual forces on the oscillatory motion. By substituting Eqs. (4), (6)–(8) into the Newton's second law of motion, namely, $\Sigma F = m(d^2x/dt^2)$, a governing equation of the oscillatory motion of working fluid with asymmetrical arrayed minichannel in the x direction yields

$$x'' + 2\zeta\omega_n x' + \omega_n^2 x = \frac{G}{m}(1 + cos\omega t) + \frac{S}{m} \tag{9}$$

where

$$\zeta = \frac{c}{2m\omega_n}, \tag{10}$$

$$\omega_n = \sqrt{\frac{k}{m}}, \tag{11}$$

$$m = V_t[\phi\rho_l + (1-\phi)\rho_v], \tag{12}$$

The governing equation, Eq. (9), is an alternative form as a single degree of freedom system subject to harmonic excitation with the variable $x(t)$. The associated boundary and initial conditions are $x(0) = 0$ and $x'(0) = 0$, respectively.

For all conditions of the oscillatory motion, an optimum design is desirable in this study. Hence in the case of the under-damped, the general solution $x(t)$, can be derived as

$$x(t) = e^{-\zeta\omega_n t}\left\{\begin{array}{l}\left\{-\frac{G}{m}\left[\frac{1}{\omega_n^2} + \frac{\omega_n^2-\omega^2}{(\omega_n^2-\omega^2)^2 + (2\zeta\omega_n\omega)^2}\right] - \frac{S}{m}\frac{1}{\omega_n^2}\right\}\cos\left[\omega_n\sqrt{(1-\zeta^2)}\right]t \\ + \left\{\frac{G}{m}\frac{-\gamma\frac{2\zeta\omega_n\omega}{(\omega_n^2-\omega^2)^2 + (2\zeta\omega_n\omega)^2} - \zeta\left[\frac{1}{\omega_n^2} + \frac{\omega_n^2-\omega^2}{(\omega_n^2-\omega^2)^2 + (2\zeta\omega_n\omega)^2}\right]}{\sqrt{(1-\zeta^2)}} - \frac{S}{m}\frac{\zeta}{\omega_n^2\sqrt{(1-\zeta^2)}}\right\}\sin\left[\omega_n\sqrt{(1-\zeta^2)}\right]t\end{array}\right\} + \left\{\frac{G}{m}\left[\frac{1}{\omega_n^2} + \frac{\omega_n^2-\omega^2}{(\omega_n^2-\omega^2)^2 + (2\zeta\omega_n\omega)^2}\cos\omega t + \frac{2\zeta\omega_n\omega}{(\omega_n^2-\omega^2)^2 + (2\zeta\omega_n\omega)^2}\sin\omega t\right] + \frac{S}{m}\frac{1}{\omega_n^2}\right\}, \tag{13}$$

where

$$\gamma = \frac{\omega}{\omega_n}. \tag{14}$$

From the foregoing expression, the parametric influences on the closed-loop PHP are investigated accordingly. The associated parameters are summarized as follows:

(1) Configurations and dimensions of the flow channel: N1, N2 and N3. To avoid the concern of stratified flow, that the interior flow channel should be less than 3 mm is appropriate. The mark N1 and N2 denote the rectangular cross-sectional area of flow channels are A_i (1×1 mm^2) and A_j (2×1 mm^2), respectively. Both N1 and N2 are constant cross-sectional area of the minichannels. The mark N3 denotes the PHP comprised of two cross-sectional areas (i.e., N1 and N2) as an asymmetrical arrayed minichannel which is shown in Fig. 1(a). The height of the three flow channels is 1 mm.
(2) Number of turns (N): 3, 6, 9, 12 and 15. The higher number of turns indicates the closed-loop PHP with longer total length.

(3) Operating temperature (T): 40, 50, 60, 70 and 80 °C. This temperature reckon on that of the adiabatic region, which is defined as

$$T = \frac{(\bar{T}_e + \bar{T}_c)}{2}. \tag{15}$$

(4) Filled liquid ratio (φ): 30%, 40%, 50%, 60% and 70%.
(5) Temperature difference between the average evaporating region and the average condensing region (ΔT): 1, 3, 5, 7 and 9 °C. ΔT is given by

$$\Delta T = \bar{T}_e - \bar{T}_c. \tag{16}$$

(6) Frequency ratio (γ): 0.1, 0.5, 1, 2 and 5.

4. Results and discussion

In the present study, the nomenclature N3 = 6 denotes the configuration and dimension of the flow channel (N3) with six (6) number of turns. The oscillatory motions for the case of the under-damped condition are shown in Fig. 2. The undamped natural frequency is often called the system's natural frequency, denoted by f_n

$$f_n = \frac{\omega_n}{2\pi}. \tag{17}$$

The abscissa and ordinate are the filled liquid ratio and system's natural frequency, respectively. It is found that system's natural frequency shows a minimum value at a filled liquid ratio around 50% for all flow channel and operating temperature. The result is ascribed to the rising the effective spring stiffness of the vapor when the filled liquid ratio is increased. It gives rise to a higher system's natural frequency when the filled liquid ratio is higher or lower than the minimum value. The larger spring stiffness implies a much larger movement of working fluid. Fig. 2 also reveals that higher system's natural frequency as well as lower damping ratio is a consequence of higher operating temperature. In addition, the closed-loop PHP with asymmetrical arrayed minichannel with lower number of turns is preferable for having a higher system's natural frequency.

Fig. 3 shows the displacement and velocity response of the closed-loop PHP with asymmetrical arrayed minichannel (N3), and operating temperature is 80 °C pertaining to the number of turns of 3 and 15, respectively. Fig. 3(a) shows the dependence of displacement response for asymmetrical arrayed minichannel for varied filled liquid ratio. It is assumed that temperature difference between the average evaporating region and the average condensing region is 5 °C and at a frequency ratio of 1. It can be seen that, for a filled liquid ratio of 30% and the number of turns of 3, the closed-loop PHP with asymmetrical arrayed minichannel has higher amplitude of the oscillatory motion. This is because a reduction of the frictional force and the elastic restoring force is encountered when the number of turns and filled liquid ratio are significantly decreased. Furthermore, the higher filled liquid ratio also raises the inertial force and reduces the oscillatory amplitude. Irrespective of the system's natural frequency being kept unchanged for the filled liquid ratio from 30% to 70%, the lower number of turns also improves rapid periodic movement as shown in Fig. 3(b). The steady oscillatory motion in terms of the displacement

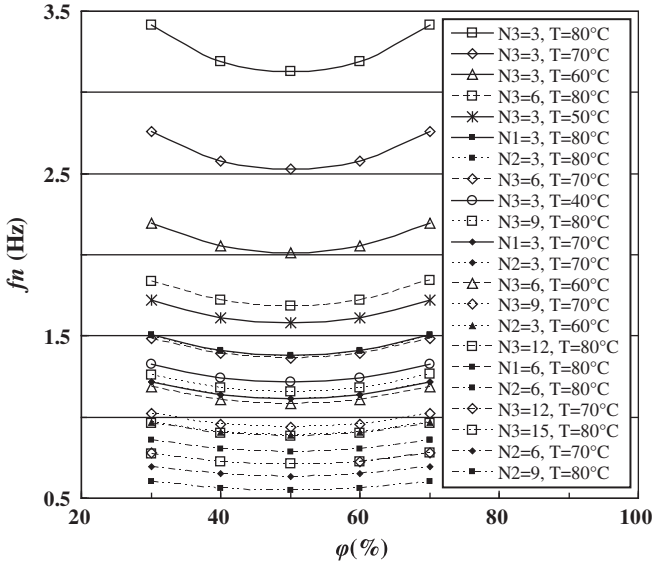

Fig. 2. Relationship of filled liquid ratio and system's natural frequency.

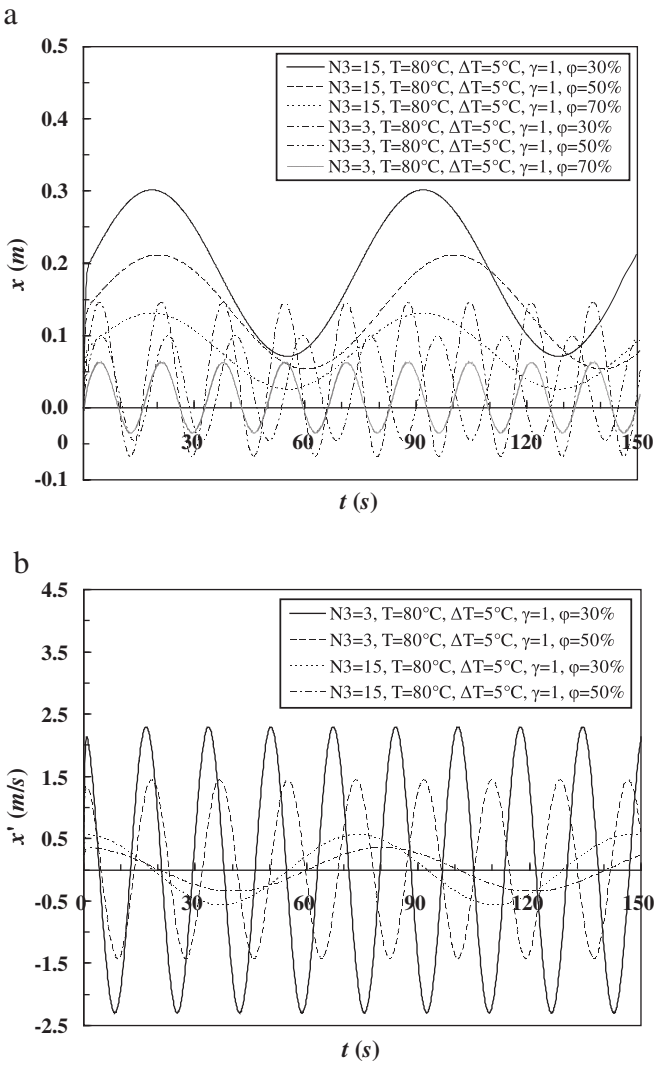

Fig. 3. Effect of number of turns on the displacement and velocity response for the asymmetrical arrayed minichannel subject to various filled liquid ratio.(a) Displacement response.(b) Velocity response.

and velocity response are established after one period operation for all under-damped cases.

Fig. 4 shows the effect of operating temperature on displacement and velocity response. As shown in Fig. 2, the asymmetrical arrayed minichannel with a number of turns of 3 has the highest system's natural frequency at an operating temperature of 80 °C. Therefore, it is clear that the oscillatory motion primarily depends on the operating temperature. In fact, the system's natural frequency increases with the rising operating temperature. This is attributed to the dramatic change of vapor density at a constant filled liquid ratio. On the other hand, with the rise of the operating temperature, an appreciable reduction of the period, and a rise of the amplitude with velocity of the oscillatory motion are also observed. The higher operating temperature contributes to decrease viscosity and latent heat of vaporization, resulting in a smaller frictional force. Nevertheless, the higher operating temperature also helps to increase thermally driven force and decreases the inertial force. Besides, higher heat input into the evaporating region also makes way in rising the operating temperature. In these regards, the foregoing interactions manage to enhance the amplitude and velocity of the oscillatory motion. However, the lower surface tension also reduces the capillary force despite the amplitude of the oscillatory motion decreases slightly.

For the effect of the number of turns on the displacement and velocity response at an operating temperature of 80 °C and a filled liquid ratio of 30%, the results are shown in Fig. 5. For a larger cross-sectional area, higher amplitude and velocity of oscillatory motion are seen due to higher thermally driven force with lower frictional force in the flow channel. The amplitude of oscillatory motion is affected by the capillary force. As shown in Fig. 5, when the number of turns is as large as 9, it has the lower and slower velocity induced by the lowest system's natural frequency for all cases. For the uniform hydraulic diameter configuration for all flow channels, lower frictional force and higher thermally driven force are expected. With the number of turns of 3 along with a filled liquid ratio of 30% at an operating temperature of 80 °C, best performance is achieved as far as oscillatory motion is concerned. The concept of flow channel applicable to asymmetric staggered array is consistent with that of Holley and Faghri [5].

Fig. 6 illustrates the influence of temperature difference between the average evaporating region and the average condensing region on the displacement and velocity response for the relations of asymmetrical arrayed minichannel. It can be observed that the amplitude and period of oscillatory motion are simply proportional to the temperature difference. With the rise of the temperature difference between the

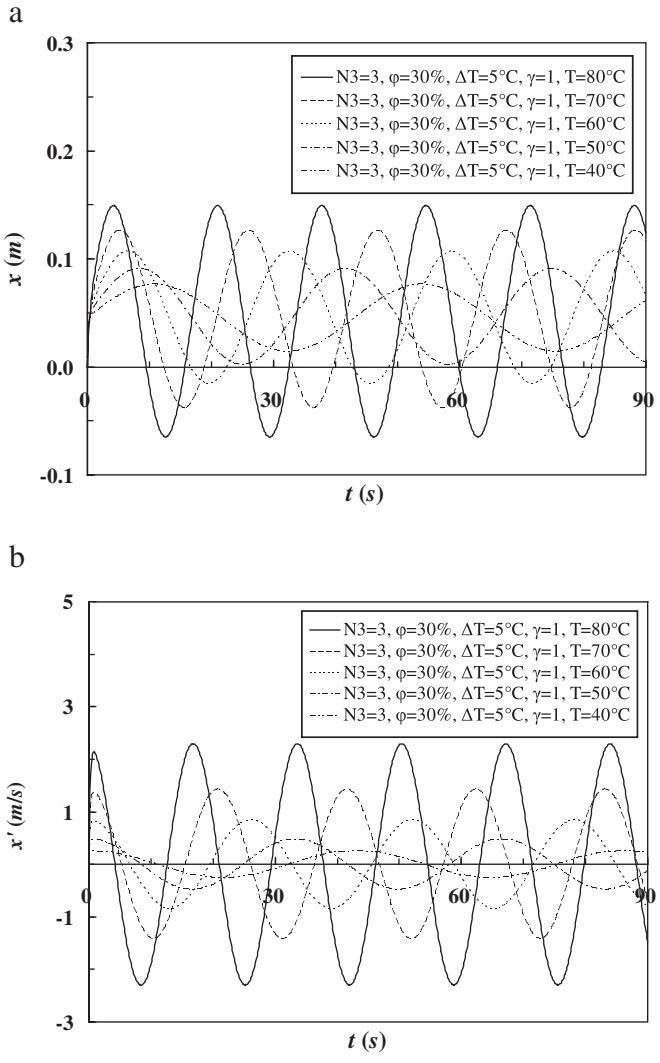

Fig. 4. Effect of operating temperature on the displacement and velocity response for the asymmetrical arrayed minichannel.(a) Displacement response.(b) Velocity response.

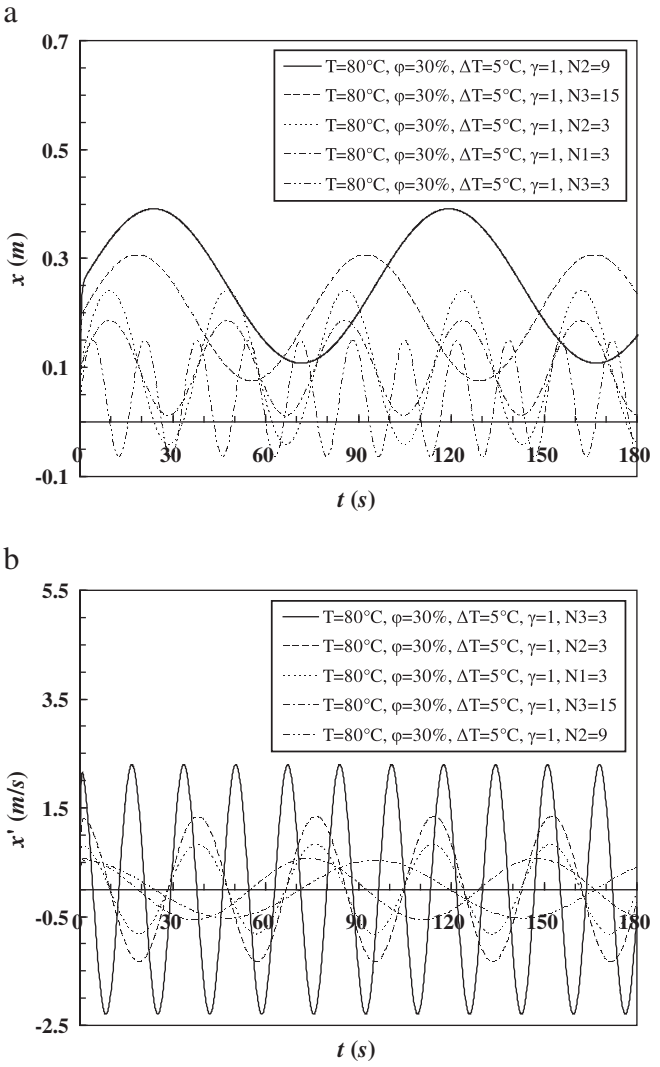

Fig. 5. Effect of configurations and dimensions on the displacement and velocity response subject to number of turns.(a) Displacement response.(b) Velocity response.

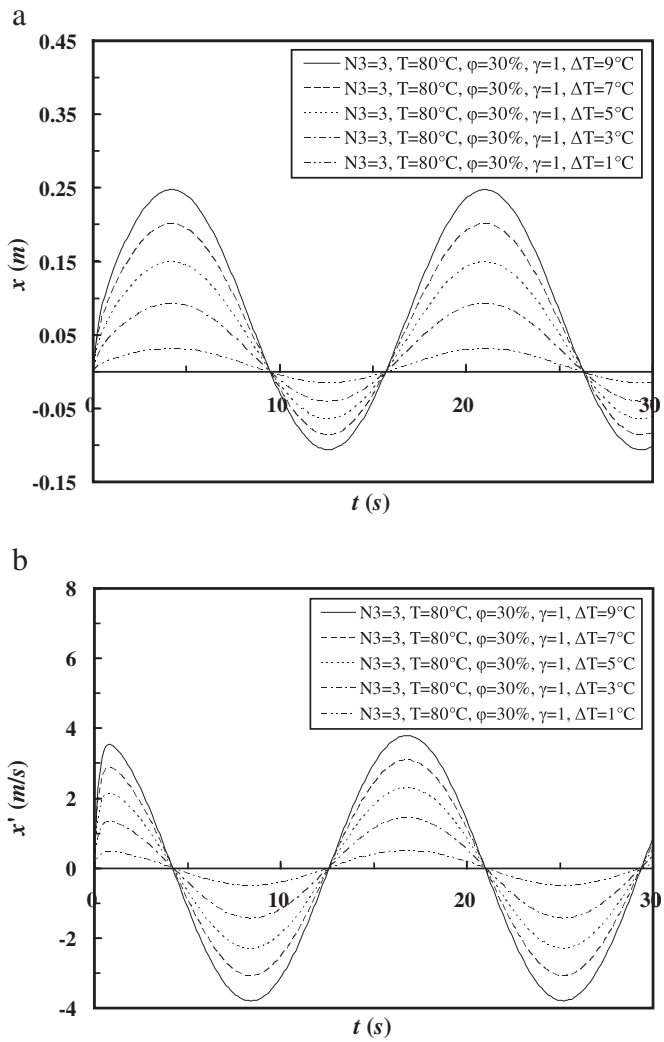

Fig. 6. Effect of temperature difference between the average evaporating region and the average condensing region on the displacement and velocity response for the asymmetrical arrayed minichannel.(a) Displacement response.(b) Velocity response.

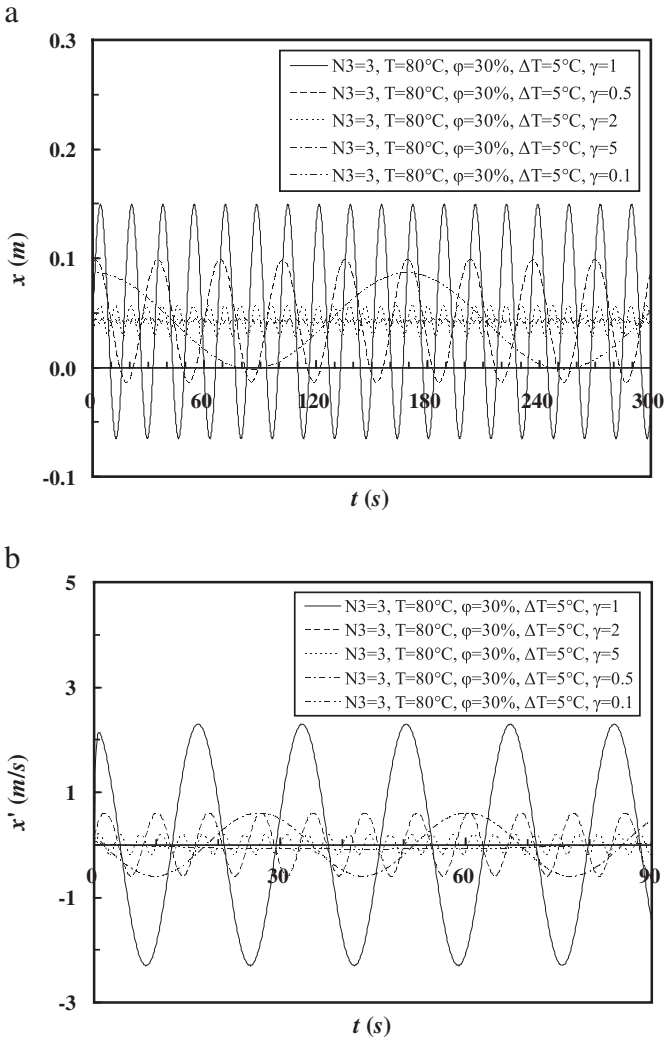

Fig. 7. Effect of frequency ratio on the displacement and velocity response for the asymmetrical arrayed minichannel.(a) Displacement response.(b) Velocity response.

average evaporating region and the average condensing region, the effect of latent heat contribution into the PHP is also increasing, leading to a substantial change of vapor volume. This phenomenon is applicable in both evaporator and condenser. As a result, the oscillatory amplitude is significantly increased.

As mentioned by Shafii et al. [11], a large proportion of the heat transfer in the PHP is contributed by sensible heat. For this purpose, the higher amplitude and the faster velocity of the oscillatory motion between the evaporating and condensing region are essential in improving the heat transfer performance. The effect of frequency ratio on the displacement and velocity response is shown in Fig. 7 with asymmetrical arrayed minichannel configuration. It is evident that the oscillatory motion becomes more pronounced when the frequency ratio is equal to 1. This is actually due to the resonance characteristic. An appreciable reduction in oscillatory magnitude is seen when the frequency is above and below 1.

5. Conclusions

The study provides a theoretical study upon the oscillatory phenomena in a horizontal closed-loop pulsating heat pipe with asymmetrical arrayed minichannel. The analytic model takes into account the temperature difference between the average evaporating region and the average condensing region as the thermally driven force for the oscillatory motion. The dominant parameters affecting the PHP such as mechanisms primarily depend on the configurations and dimensions of the flow channel, the number of turns, the filled liquid ratio, the frequency ratio, the operating temperature, and the temperature difference between the average evaporating region and the average condensing region are investigated in this study. The calculated results show that the closed-loop pulsating heat pipe with asymmetrical arrayed minichannel with lower number of turns, lower filled liquid ratio, higher operating temperature and higher temperature difference between the average evaporating region and the average condensing region for the frequency ratio of unity could achieve a better performance due to larger oscillatory motions.

Acknowledgements

The authors are indebted to the the Energy R&D foundation funding from the Bureau of Energy of the Ministry of Economic Affairs, Taiwan.

References

[1] H. Akachi, US Patent No. 4921041, 1990.
[2] Q. Cai, C.L. Chen, J.F. Asfia, Operating characteristic investigations in pulsating heat pipe, Journal of Heat Transfer 128 (12) (2006) 1329–1334.

[3] X.M. Zhang, J.L. Xu, Z.Q. Zhou, Experimental study of a pulsating heat pipe using FC-72, ethanol, and water as working fluids, Experimental Heat Transfer 17 (1) (2004) 47–67.
[4] P. Charoensawan, P. Terdtoon, Thermal performance of horizontal closed-loop oscillating heat pipes, Applied Thermal Engineering 28 (5–6) (2008) 460–466.
[5] B. Holley, A. Faghri, Analysis of pulsating heat pipe with capillary wick and varying channel diameter, International Journal of Heat and Mass Transfer 48 (13) (2005) 2635–2651.
[6] J.S. Kim, Y.B. Im, N.H. Bui, Numerical analysis of pulsating heat pipe based on separated flow model, Journal of Mechanical Science and Technology 19 (9) (2005) 1790–1800.
[7] Z. Lin, S. Wang, J. Huo, Y. Hu, J. Chen, W. Zhang, E. Lee, Heat transfer characteristics and LED heat sink application of aluminum plate oscillating heat pipes, Applied Thermal Engineering 31 (14–15) (2011) 2221–2229.
[8] H.B. Ma, M.A. Hanlon, C.L. Chen, An investigation of oscillating motions in a miniature pulsating heat pipe, Microfluidics and Nanofluidics 2 (2) (2006) 171–179.
[9] K.R. Narasimha, S.N. Sridhara, M.S. Rajagopal, K.N. Seetharamu, Parametric studies on pulsating heat pipe, International Journal of Numerical Methods for Heat and Fluid Flow 20 (4) (2010) 392–415.
[10] P. Sakulchangsatjatai, P. Terdtoon, T. Wongratanaphisan, P. Kamonpet, M. Murakami, Operation modeling of closed-end and closed-loop oscillating heat pipes at normal operating condition, Applied Thermal Engineering 24 (7) (2004) 995–1008.
[11] M.B. Shafii, A. Faghri, Y. Zhang, Thermal modeling of unlooped and looped pulsating heat pipes, Journal of Heat Transfer 123 (6) (2001) 1159–1172.
[12] M.B. Shafii, A. Faghri, Y. Zhang, Analysis of heat transfer in unlooped and looped pulsating heat pipes, International Journal of Numerical Methods for Heat and Fluid Flow 12 (5) (2002) 585–609.
[13] Y. Zhang, A. Faghri, Oscillatory flow in pulsating heat pipes with arbitrary numbers of turns, Journal of Thermophysics and Heat Transfer 17 (3) (2003) 340–347.
[14] Y. Zhang, A. Faghri, Advances and unsolved issues in pulsating heat pipes, Heat Transfer Engineering 29 (1) (2008) 20–44.
[15] H.M. Hofmann, R. Kaiser, M. Kind, H. Martin, Calculations of steady and pulsating impinging jets—an assessment of 13 widely used turbulence models, Numerical Heat Transfer Part B 51 (6) (2007) 565–583.
[16] T. Demircan, H. Turkoglu, The numerical analysis of oscillating rectangular impinging jets, Numerical Heat Transfer Part A 58 (2) (2010) 146–161.
[17] Y.L. Yen, P.C. Huang, C.F. Yang, Y.J. Chen, Numerical study of heat transfer of a porous-block-mounted heat source subjected to pulsating channel flow, Numerical Heat Transfer Part A 54 (4) (2008) 426–449.
[18] S.M. Aminossadati, B. Ghasemi, Comparison of mixed convection in a square cavity with an oscillating versus a constant velocity wall, Numerical Heat Transfer Part A 54 (7) (2008) 726–743.
[19] A. Faghri, Heat Pipe Science and Technology, Taylor & Francis, Washington, DC, 1995, p. 65.